

SCIENTIFIC REPORTS



OPEN

Thrombomodulin regulates monocyte differentiation *via* PKC δ and ERK1/2 pathway *in vitro* and in atherosclerotic artery

Received: 23 May 2016
Accepted: 08 November 2016
Published: 02 December 2016

Chien-Sung Tsai^{1,2,3,4,*}, Yi-Wen Lin^{1,2,5,*}, Chun-Yao Huang^{2,6}, Chun-Min Shih^{2,6}, Yi-Ting Tsai¹, Nai-Wen Tsao⁷, Chin-Sheng Lin⁸, Chun-Che Shih⁹, Hellen Jeng¹⁰ & Feng-Yen Lin^{2,6}

Thrombomodulin (TM) modulates the activation of protein C and coagulation. Additionally, TM regulates monocyte migration and inflammation. However, its role on monocyte differentiation is still unknown. We investigated the effects of TM on monocyte differentiation. First, we found that TM was increased when THP-1 cells were treated with phorbol-12-myristate-13-acetate (PMA). Overexpression of TM enhanced the macrophage markers, CD14 and CD68 expression in PMA-induced THP-1. TM siRNA depressed the PMA-induced increase of p21^{Cip1/WAF1} via ERK1/2-NF-kB p65 signaling. TM regulated cytoskeletal reorganization via its interaction with paxillin, cofilin, LIMK1, and PYK2. In addition, PMA-induced p21^{Cip1/WAF1} expression, CD14-positive cell labeling intensity and ERK1/2 phosphorylation were markedly inhibited when protein kinase C- δ (PKC δ) was knocked down. We identified that TM directly interacts with PKC δ . PKC δ was highly expressed in human atherosclerotic arteries and colocalized with TM in CD68-positive infiltrated macrophages of plaques, indicating that the coordination between TM and PKC δ in macrophages participated in atherogenesis. TM may act as a scaffold for PKC δ docking, which keeps PKC δ in the region close to the monocyte membrane to promote the activation of ERK1/2. Taken together, our findings suggest that TM-PKC δ interaction may contribute to cardiovascular disorders by affecting monocyte differentiation, which may develop future therapeutic applications.

Monocytes undergo transendothelial migration and differentiate into macrophages¹, which take on the morphology and functional properties that are characteristic of the tissue they enter². Atherosclerosis is considered as both a chronic inflammatory disease and a lipid metabolism disorder in which macrophages are responsible for intracellular lipid accumulation as well as foam cell formation in early atherosclerotic lesions^{3–5}. After the induction of hyperlipidemia and in response to chemotactic factors, monocytes exit the peripheral bloodstream and then enter the arterial intima, where they further differentiate into macrophages after exposure to environmental factors, such as oxidized low-density lipoprotein (oxLDL), *Chlamydia pneumoniae*, and macrophage growth factors^{6–8}. In addition, macrophages contribute to atherosclerotic lesion development through the production and release of a variety of soluble mediators, such as chemokines, cytokines, growth factors, and reactive oxygen species⁹. Furthermore, macrophages also play roles in plaque disruption and vascular remodeling in atherosclerosis by releasing matrix-degrading proteinases as well as their activators and inhibitors¹⁰. A previous paper showed that atherosclerotic lesions are fewer and smaller in apoE-deficient mice that completely lack macrophage

¹Division of Cardiovascular Surgery, Tri-Service General Hospital, National Defense Medical Center, Taipei, Taiwan.

²Division of Cardiology and Cardiovascular Research Center, Taipei Medical University Hospital, Taipei, Taiwan.

³Department and Graduate Institute of Pharmacology, National Defense Medical Center, Taipei, Taiwan. ⁴Division of Cardiovascular Surgery, Department of Surgery, Taoyuan Armed Forces General Hospital, Taoyuan, Taiwan.

⁵Institute of Oral Biology, National Yang-Ming University, Taipei, Taiwan. ⁶Departments of Internal Medicine, College of Medicine, School of Medicine, Taipei Medical University, Taipei, Taiwan. ⁷Division of Cardiovascular Surgery, Taipei Medical University Hospital, Taipei, Taiwan. ⁸Division of Cardiology, Tri-Service General Hospital, National Defense Medical Center, Taipei, Taiwan. ⁹Division of Cardiovascular Surgery, Taipei Veterans General Hospital, Taipei, Taiwan.

¹⁰Division of Anatomy and Cell Biology, College of Medicine, School of Medicine, Taipei Medical University, Taipei, Taiwan. *These authors contributed equally to this work. Correspondence and requests for materials should be

addressed to F.-Y.L. (email: g870905@tmu.edu.tw)

colony-stimulating factor (M-CSF), an important promoter of macrophage differentiation, compared to mice deficient in only apoE¹¹, confirming that macrophage differentiation is a critical component of atherogenesis⁹. Hence, the prevention of macrophage differentiation could confer protection from atherosclerosis with multiple pathologic effects.

Human THP-1 monocytic cells can be induced to differentiate into macrophages by treatment with phorbol-12-myristate-13-acetate (PMA), after which they can be converted into foam cells by exposure to oxLDL¹². Schwende *et al.* reported that the differentiation statuses of THP-1 cells that were induced by PMA and 1,25-dihydroxyvitamin D3 are different. PMA treatment, which activates protein kinase C (PKC), induces a greater degree of differentiation in THP-1 cells, as is reflected by their increased adherence and expression of macrophage differentiation-associated surface markers¹³. PKCs, a family of serine/threonine kinases, play important roles in several signal transduction cascades and are known to be involved in inflammation, cell growth, and migration¹⁴. The PKC family consists of fifteen isozymes in humans. In addition to its classic (α , β I, β II, γ) and novel (δ , ϵ , η , θ) members, the PKC family includes two atypical members (ξ , λ) that are distinguished structurally by the presence of only one PKC zinc finger module in their regulatory domain and biochemically by their inability to bind to and respond to phorbol esters and diacylglycerol^{15,16}.

Thrombomodulin (TM), a glycosylated type I transmembrane protein¹⁷, was first discovered on endothelial cells, where the TM/thrombin complex has been shown to modulate the activation of protein C and the inactivation of coagulation¹⁸. In 2008, recombinant human soluble thrombomodulin (rTM) was approved for the treatment of disseminated intravascular coagulation in Japan. TM is also expressed on keratinocytes¹⁹, megakaryocytes, platelets²⁰, and monocytes²¹, indicating that TM has additional functions in addition to its role as an anticoagulant. It has been hypothesized that TM also functions as an angiogenic factor²², an adhesion molecule²³, and an anti-inflammatory agent^{24,25}. Moreover, our previous study demonstrated that down-regulation of TM in monocytes is associated with TNF- α production and poor early outcomes in patients following serious surgery²⁶. Knockdown of TM enhanced IL-6-induced migration and chemotaxis in monocytes, indicating that TM plays important roles in monocyte functions²⁷. A previous study²⁸ reported that exposure of THP-1 cells to recombinant human soluble thrombomodulin (rTM) induced growth arrest and differentiation in THP-1 cells by activating JNK/c-Jun signaling, suggesting that rTM is a positive regulator of THP-1 differentiation. Although it has been suggested that TM is a potent stimulator of monocyte migration and differentiation, the roles of endogenous TM in THP-1 differentiation and its regulating mechanisms are not yet fully understood. Thus, the aim of this study was to investigate the mechanism of action underlying the effects of TM on PMA-induced monocyte differentiation.

Here, we demonstrate that TM expression was increased during PMA-induced THP-1 cell differentiation. Furthermore, we suggested that the mechanisms underlying TM-regulated monocyte differentiations are likely to be mediated through a direct interaction with PKC δ , which is thought to induce ERK1/2 activation and to cause THP-1 cell differentiation. This study may provide a new view of the role of endogenous TM in macrophage differentiation in atherogenesis.

Results

Thrombomodulin was associated with PMA-induced monocytic THP-1 cell differentiation.

TM is expressed on the surface of monocytes and is important for the regulation of THP-1 cell migration²⁷. We wanted to determine whether TM is also involved in monocyte differentiation. We first determined the expression of TM during PMA-induced THP-1 cell differentiation into macrophages. The data indicated that treatment of THP-1 cells with 150 nM PMA for 24–72 h markedly increased the expression of TM in a time-dependent manner (Fig. 1A), suggesting that TM played a role in PMA-induced monocytic THP-1 cell differentiation. Cell adhesion and Liu staining were used to verify THP-1 cell differentiation. The quantitative data showed that treatment of THP-1 cells with PMA for 72 h significantly induced differentiation by $43.2 \pm 6.9\%$ (2160 ± 345 differentiated cells/per 5000 THP-1 cells) relative to the untreated control group ($5.1 \pm 2.5\%$; 255 ± 125 differentiated cells/per 5000 THP-1 cells; Fig. 1B). To verify that TM contributed to the effects of PMA-induced THP-1 cell differentiation, THP-1 cells were transfected with either TM siRNA for knockdown or HA-TM FL plasmid for overexpression for 24 h, which was followed by PMA treatment for 72 h. The results showed that knockdown of TM significantly decreased PMA-induced monocyte differentiation by $26.1 \pm 4.5\%$ (1305 ± 225 differentiated cells/per 5000 THP-1 cells). In contrast, overexpression of TM followed by PMA treatment significantly enhanced THP-1 cell differentiation by $95.4 \pm 9.9\%$ (4770 ± 495 differentiated cells/per 5000 THP-1 cells; Fig. 1B). The THP-1 cells were harvested, and the macrophage surface markers CD14 and CD68 were analyzed using immunostaining and flow cytometry. As shown in Fig. 1C,D, these cell surface antigens were strongly induced by $259.7 \pm 24.3\%$ for CD14 and $265.8 \pm 19.4\%$ for CD68 after the THP-1 cells were exposed to PMA to induce differentiation. siRNA knockdown of TM markedly decreased PMA-induced expression of CD14 by $116.4 \pm 12.4\%$ and CD68 by $123.9 \pm 9.5\%$ relative to the PMA-treated group. Conversely, the levels of CD14 and CD68 were significantly increased by $334.6 \pm 20.1\%$ and $388.9 \pm 30.4\%$, respectively, when THP-1 cells were transfected with HA-TM FL plasmid followed by PMA stimulation. Hence, down-regulation of TM markedly reduced and up-regulation of TM greatly enhanced the macrophage-like phenotypes that were induced by PMA treatment. Additionally, transfection of THP-1 cells with TM siRNA or HA-TM FL plasmid alone did not increase the CD14 and CD68 expression. These data suggest that TM was involved in PMA-induced THP-1 cell differentiation. The flow cytometry and western blot analysis were used to define the efficiency of TM siRNA and HA-TM FL plasmid (Fig. 1E,F).

TM modulates p21^{Cip1/WAF1} expression via ERK1/2 signaling, which reduces cell growth during PMA-induced THP-1 cell differentiation. TM contributes to the effects of PMA-induced THP-1 cell differentiation; the molecular mechanisms involved in TM-mediated differentiation were therefore investigated.

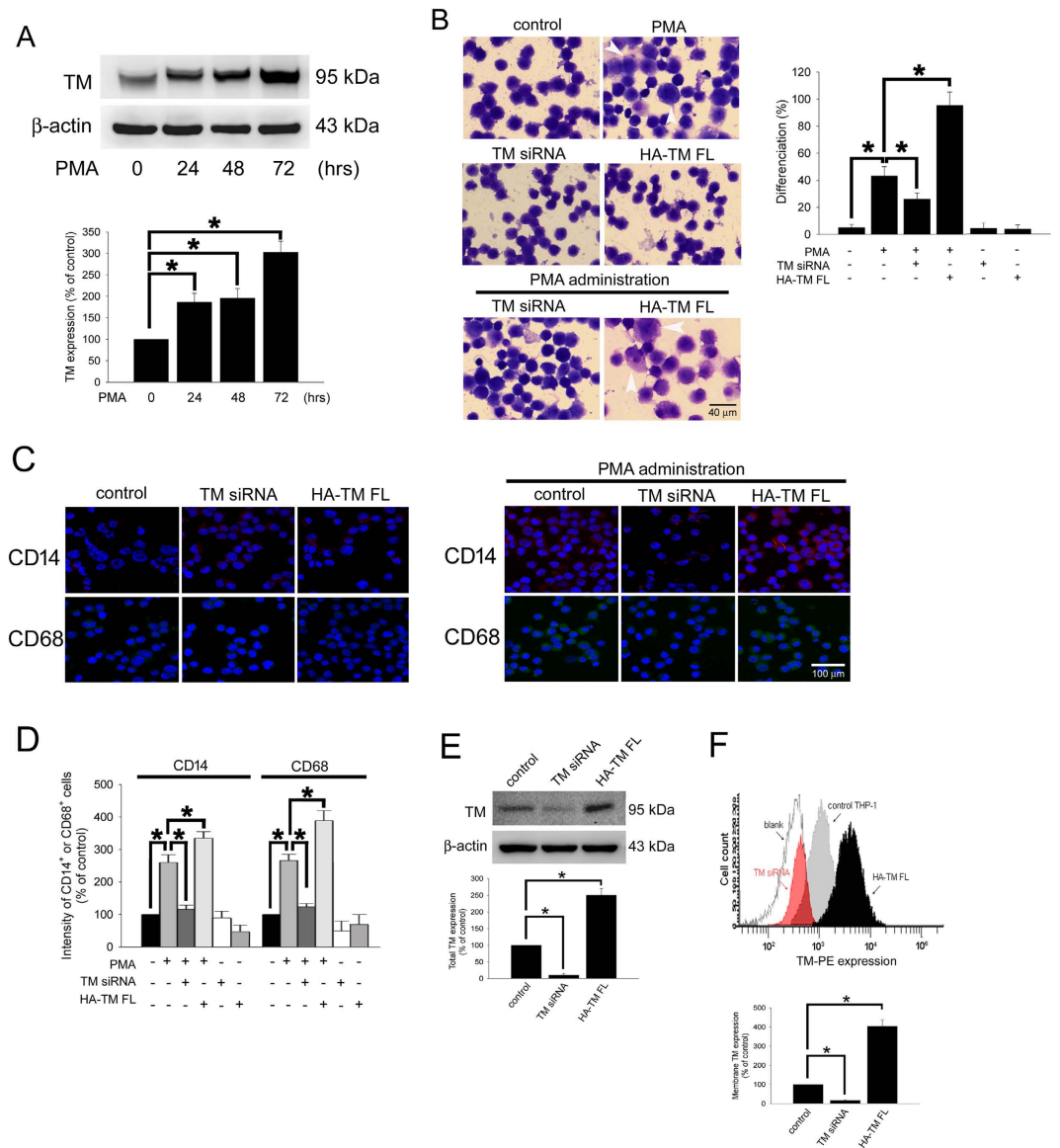


Figure 1. PMA-induced TM expression mediates morphological changes and differentiation marker expression in THP-1 cells. (A) THP-1 cells were treated with 150 nM PMA for 24–72 hours. The total cell lysates were harvested, and the expression of TM was analyzed using western blot analysis. β -actin was used as a loading control. Five independent experiments have been performed ($n = 5$) and representative images have been showed. The amount of proteins expression was quantified using densitometry and presented as bar graph. The data are presented as the mean \pm SD ($n = 5$), and $*p < 0.05$ was considered significant. (B) THP-1 cells were transfected with TM siRNA or HA-TM FL plasmid for 24 h followed by PMA stimulation for 72 hours. The morphology of the cells was observed using light microscopy. The adherent differentiated macrophage-like cells are indicated by a white arrowhead. Five independent experiments have been performed ($n = 5$). The quantification is shown in the right graph. (C) The expression of the macrophage cell surface markers CD14 (red) and CD68 (green) was analyzed using immunofluorescence and microscopy. Hoechst staining was used to label the nuclei. The scale bar indicates 100 μ m. Five independent experiments have been performed ($n = 5$), and showed representative images. (D) The expression of CD14 and CD68 was analyzed using flow cytometry. Data are expressed as a % of the control, are presented as the mean \pm SD and represent the results of three independent experiments ($n = 3$, $*p < 0.05$ was considered significant). (E) THP-1 cells were transfected with TM siRNA or HA-TM FL plasmid for 24 h, the TM in total cell lysate was analyzed using western blot analysis. The amount of proteins expression was quantified using densitometry and presented as bar graph. (F) The membrane TM was stained by PE-conjugated anti-TM antibody and analyzed using flow cytometry. The relative amount of membrane TM expression was presented as bar graph. The data are presented as the mean \pm SD ($n = 5$), and $*p < 0.05$ was considered significant.

Reduced cell growth is known to be coupled to the differentiation process, and the cell cycle inhibitor p21^{Cip1/WAF1} is responsible for the early stages of the differentiation program^{29,30}. The marker p21^{Cip1/WAF1} inhibits cell cycle

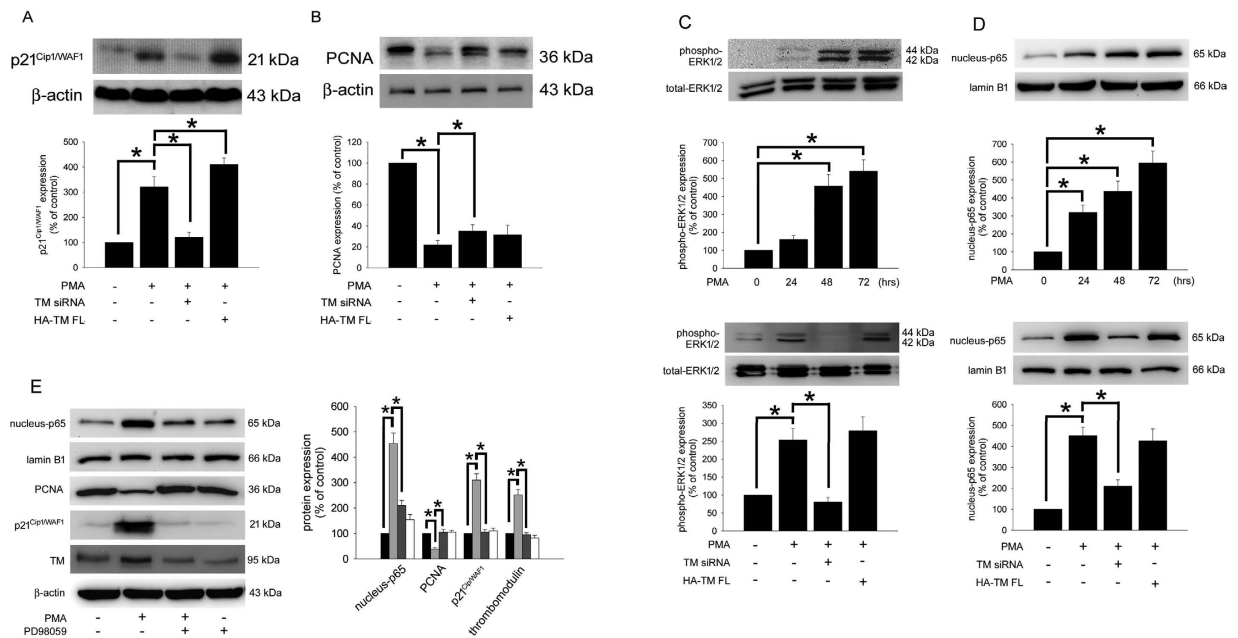


Figure 2. TM regulates PCNA and p21^{Cip1/WAF1} expression via ERK1/2 activation in PMA-stimulated THP-1 cells. (A,B) THP-1 cells were transfected with TM siRNA or HA-TM FL plasmid for 24 h, which was followed by PMA stimulation for 72 h. The expression of p21^{Cip1/WAF1} and PCNA in total cell lysates was assayed using western blot analysis. (C, upper and D, upper) THP-1 cells were stimulated with 150 nM PMA for 24–72 h. The expression of phosphorylated ERK1/2 in total cell lysates and NF-κB p65 in nuclear fraction were assayed using western blot analysis. (C, lower and D, lower), THP-1 cells were transfected with TM siRNA or HA-TM FL plasmid for 24 h, which was followed by PMA stimulation for 72 h. The expression of phosphorylated ERK1/2 and NF-κB p65 was assayed using western blot analysis. (E) THP-1 cells were pretreated with 10 μM PD98059 for 1 h followed by PMA treatment (dark gray) or treated with PD98059 only (white) for 72 h (black: naïve THP-1 cells; light gray: PMA treatment). A western blot assay was performed to determine the expression of NF-κB p65 (nuclear fraction), PCNA, and p21^{Cip1/WAF1} (total cell lysates). Lamin B1, total ERK1/2, and β-actin were used as the loading controls, as indicated. Five independent experiments have been performed (n = 5) for all studies, and representative images have been showed. The density of each band was quantified using densitometry and related protein expression was presented as bar graph. The data are presented as the mean ± SD, and *p < 0.05 was considered significant.

	control	TM si RNA	HA-TM FL	PMA administration for 5 days		
				—	TM si RNA	HA-TM FL
G ₀ /G ₁ phase	19.6 ± 2.8%	20.5 ± 3.2%	18.7 ± 3.1%	70.3 ± 2.9%*	47.3 ± 3.7%†	84.1 ± 1.9%*†
S phase	58.9 ± 6.2%	54.2 ± 5.0%	53.4 ± 7.0%	8.9 ± 3.1%*	29.7 ± 5.2%†	11.2 ± 3.5%*
G ₂ /M phase	16.2 ± 8.8%	25.3 ± 9.1%	27.9 ± 3.4%	10.6 ± 0.8%*	6.2 ± 1.0%*	4.5 ± 1.9%*

Table 1. The DNA content of THP-1 cells in PMA administration for 5 days. (n = 5). *p < 0.05 compared to control group; †p < 0.05 compared to PMA-administrated group.

progression by binding to proliferating cell nuclear antigen (PCNA) and blocking the ability of PCNA to activate DNA polymerase δ, the principal replicative DNA polymerase^{31,32}. Therefore, levels of p21^{Cip1/WAF1} were determined and used as a differentiation index. The level of PCNA was also determined. As shown in Fig. 2A,B, stimulating THP-1 cells with PMA induced p21^{Cip1/WAF1} and inhibited PCNA expression relative to the untreated group (Fig. 2A,B, lane 2). To explore whether TM-associated signaling contributed to the effects of PMA treatment on p21^{Cip1/WAF1} expression, the cells were knocked down using TM siRNA prior to PMA treatment. The data showed that the level of p21^{Cip1/WAF1} was markedly decreased, and the level of PCNA was increased (Fig. 2A,B, lane 3). Conversely, the level of p21^{Cip1/WAF1} was increased when cells were transfected with HA-TM FL followed by PMA treatment (Fig. 2A, lane 4), suggesting that TM contributed to the effects of PMA-induced p21^{Cip1/WAF1} expression in THP-1 cells. Furthermore, reduced cell growth/cell cycle arrest was also confirmed using flow cytometry, and treatment of cells with PMA for 5 days significantly induced cell cycle arrest. The percentage of cells in G₀-G₁ was 70.3 ± 2.9% compared to 19.6 ± 2.2.8% in the untreated control group. Transfecting cells with TM siRNA prior to PMA treatment significantly decreased the percentage of G₀-G₁ cells by 47.3 ± 3.7% relative to the PMA-treated group. The percentage of G₀-G₁ cells was enhanced to 84.1 ± 1.9% when THP-1 cells were transfected with HA-TM-FL followed by PMA treatment (Table 1), indicating that p21^{Cip1/WAF1} expression, which was modulated by

	control	PD98059	PMA administration for 5 days	
			—	PD98059
G ₀ /G ₁ phase	19.6 ± 2.8%	20.5 ± 3.1%	70.3 ± 2.9%*	40.9 ± 5.4%*†
S phase	58.9 ± 6.2%	60.1 ± 7.5%	8.9 ± 3.1%*	15.9 ± 2.8%*†
G ₂ /M phase	16.2 ± 8.8%	15.7 ± 6.8%	10.6 ± 0.8%*	43.2 ± 5.1%*

Table 2. The effects of ERK1/2 inhibitors in PMA-administrated THP-1 cells. (n = 5). PD98059, ERK1/2 inhibitor. *p < 0.05 compared to control group; †p < 0.05 compared to PMA-administrated group.

TM, promoted a reduction in cell growth in PMA-induced THP-1 cells. The mechanism by which TM regulates p21^{Cip1/WAF1} expression in PMA-stimulated THP-1 cells was then studied. The data demonstrated that exposing THP-1 cells to 150 nM PMA induced ERK1/2 phosphorylation (Fig. 2C, upper). Knockdown of TM using siRNA prior to PMA treatment inhibited ERK1/2 phosphorylation. The level of ERK1/2 phosphorylation was slightly increased when cells were transfected with HA-TM FL prior to PMA treatment (Fig. 2C, lower), suggesting that ERK1/2 phosphorylation, which is involved in PMA-induced THP-1 cell differentiation, is regulated by TM. NF-κB is one possible downstream signaling molecule of ERK1/2³³. Therefore, western blot analysis for nuclear NF-κB p65 was also performed. Similar to ERK1/2 activation, nuclear NF-κB p65 is involved in PMA-induced THP-1 cell differentiation, which is regulated by TM (Fig. 2D). As shown in Fig. 2E, even though treatment of PD98059 alone for 72 hours did decrease the endogenous expression of TM in THP-1 cells, differentiation induced by PMA markedly increased p65 levels in the nucleus and p21^{Cip1/WAF1} expression, blockade of ERK1/2 using PD98059 abrogated the PMA-induced increase in p65 levels in the nucleus and p21^{Cip1/WAF1} expression, suggesting that TM-ERK1/2-NF-κB- and p65-mediated signaling played a crucial role in PMA-induced p21^{Cip1/WAF1} and PMA-decreased PCNA expression in THP-1 cells. In additions, as shown in Table 2, flow cytometry data indicated that the percentage of cells in G₀-G₁ significantly decreased to 40.9 ± 5.4% in the group pretreated with PD98059 followed by PMA stimulation relative to 70.3 ± 2.9% in the only PMA-treated group, confirming that ERK1/2 indeed played an important role in the PMA-induced reduction in cell growth. Finally, we analyzed the effects of PD98059 alone on THP-1 differentiation. It showed that treatment of PD98059 for 5 days did not change the rhythm of the cell cycle on THP-1 cells. The above results indicate that TM modulated p21^{Cip1/WAF1} expression via ERK1/2-NF-κB p65 signaling, which further promoted a reduction in cell growth, which is coupled to the differentiation process in PMA-induced THP-1 cells.

TM interacted with and promoted the activation of cytoskeleton-associated molecules via ERK1/2 signaling during PMA-induced THP-1 cell differentiation. The cytoskeleton is the key component that regulates cell migration and differentiation³⁴. To study the activation of cytoskeleton-associated molecules during THP-1 cell differentiation, western blot analysis for different phosphorylated forms of cytoskeleton-associated scaffolding proteins was performed. As shown in Fig. 3A, inducing differentiation with PMA markedly induced paxillin, cofilin, LIMK1, and PYK2 phosphorylation (Fig. 3A, lane 2) relative to levels in the untreated group. To determine whether TM contributes to these effects, TM expression was knocked down using TM siRNA prior to PMA treatment. The results showed that TM knockdown significantly inhibited paxillin, cofilin, LIMK1, and PYK2 phosphorylation (Fig. 3A, lane 3), suggesting that TM was also responsible for PMA-induced activation of cytoskeleton-associated molecules during THP-1 cell differentiation. Overexpression of TM followed by PMA treatment slightly increased the activation of these molecules relative to the only PMA-treated group (Fig. 3A, lane 4). To determine whether ERK1/2-mediated signaling also played roles in PMA-induced activation of cytoskeleton-associated molecules during THP-1 cell differentiation, THP-1 cells were pretreated with PD98059 followed by PMA stimulation. We found that the phosphorylation of paxillin, cofilin, LIMK1, and PYK2 was inhibited relative to the PMA-treated group (Fig. 3B, lane 3), suggesting that ERK1/2 signaling, which was responsible for PMA-induced p21^{Cip1/WAF1} expression, also played a crucial role in the activation of cytoskeleton-associated molecules during PMA-induced THP-1 cell differentiation. To determine whether TM interacts with these molecules in cells, immunoprecipitation (IP) assays were performed. As shown in Fig. 3C, IP-western analysis demonstrated that paxillin, cofilin, LIMK1, and PYK2 were present in the anti-TM antibody-immunoprecipitated fractions isolated from PMA-treated THP-1 cells (Fig. 3C lane 2), suggestion that TM can directly interact with cytoskeleton-associated molecules in PMA-stimulated THP-1 cells. In order to confirm the results of IP-western analysis, subcellular distributions of TM and cytoskeletons in THP-1 cells were detected by immunofluorescence and observed by confocal microscopy. Confocal microscopy showed that TM was predominantly found in the membrane of cells, and that naïve cells with dispersed distribution of PYK2 and cofilin (Fig. 3D). Interestingly, PMA may trigger a distribution change of cytoplasmic PYK2 and cofilin and make a colocalization with TM in THP-1 cells (Fig. 3E). These results suggested that TM directly interacts with and modulates paxillin, cofilin, LIMK1, and PYK2 phosphorylation via ERK1/2 signaling during PMA-induced THP-1 cell differentiation.

PKCδ interacts with TM to regulate PMA-induced THP-1 cell differentiation. In the above-described data, we show that TM and ERK signaling are associated with PMA-induced THP-1 cell differentiation. We identified a signaling pathway that links TM to ERK1/2 signaling and that induced both p21^{Cip1/WAF1} expression and the activation of cytoskeleton-associated proteins. However, the details of the molecular mechanisms that mediate TM's function during ERK1/2 activation were not fully clear and were therefore explored. Increasing evidence has revealed that PMA treatment activates PKC and that it induces a greater degree of differentiation in THP-1

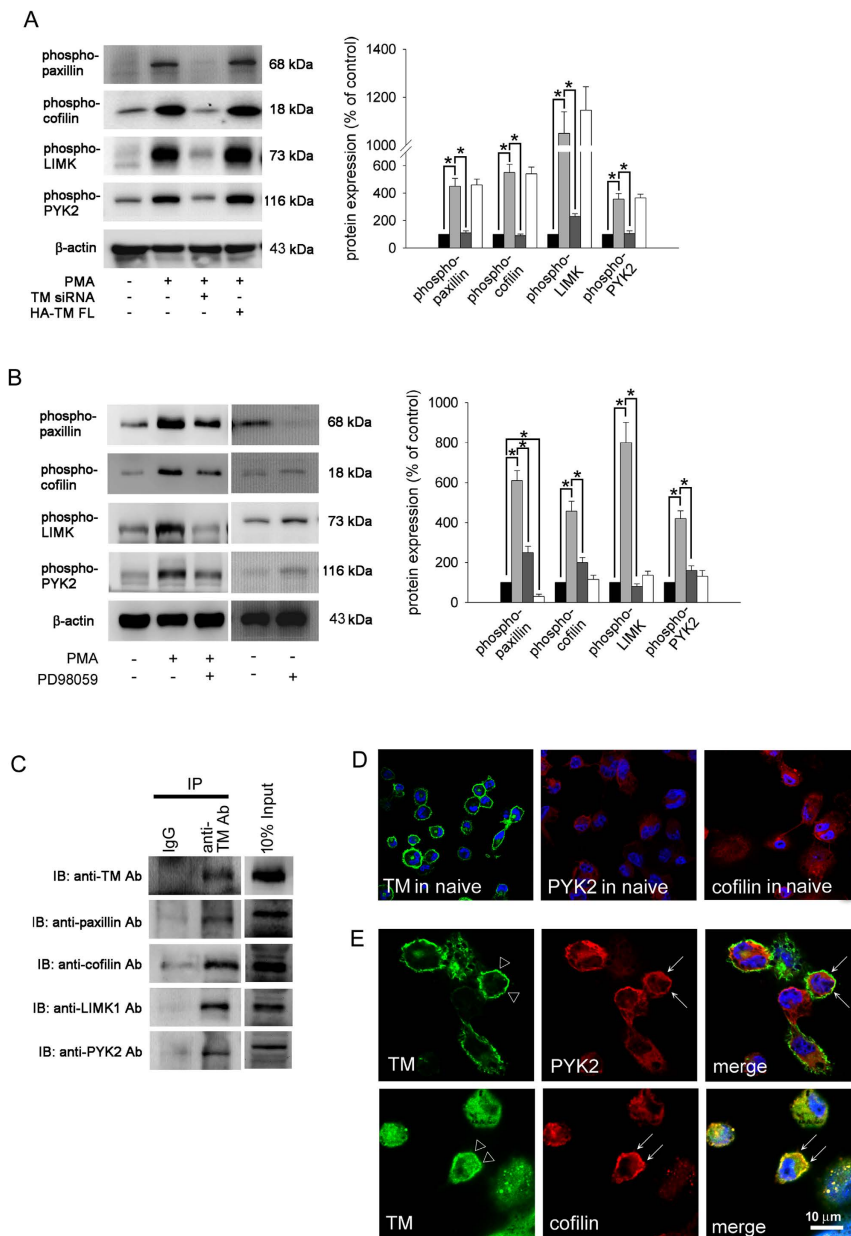


Figure 3. TM interacts with and activates cytoskeleton-associated molecules through ERK1/2 signaling in PMA-stimulated THP-1 cells. (A) THP-1 cells were transfected with TM siRNA (dark gray) or HA-TM FL plasmid for 24 h followed by PMA stimulation for 72 hours (black: naïve THP-1 cells; light gray: PMA treatment). The total cell lysates were purified and analyzed for the activation (phosphorylation) of paxillin, cofilin, LIMK1, and PYK2 using western blot analysis. β -actin was used as a loading control. Five independent experiments have been performed ($n = 5$) for all studies, and representative images have been showed. The density of each band was quantified using densitometry and related protein expression was presented as bar graph. The data are presented as the mean \pm SD, and $*p < 0.05$ was considered significant. (B) THP-1 cells were pretreated with $10 \mu\text{M}$ PD98059 (dark gray) for 1 h followed by PMA treatment for 72 hours (black: naïve THP-1 cells; light gray: PMA treatment; white: only PD98059 treatment). The total cell lysates were purified and analyzed for the activation (phosphorylation) of paxillin, cofilin, LIMK1, and PYK2 using western blot analysis. β -actin was used as a loading control. Five independent experiments have been performed ($n = 5$) for all studies, and representative images have been showed. The density of each band was quantified using densitometry and related protein expression was presented as bar graph. The data are presented as the mean \pm SD, and $*p < 0.05$ was considered significant. (C) Lysates of THP-1 cells were immunoprecipitated using an anti-TM antibody or a rabbit IgG control followed by immunoblotting with antibodies against TM, paxillin, cofilin, LIMK1, or PYK2, as indicated. Five independent experiments have been performed for all studies ($n = 5$), and representative images have been showed. (D) Subcellular distributions of TM, PYK2 and cofilin in naïve THP-1 cells were detected by immunofluorescence and observed by confocal microscopy. (E) THP-1 cells were treated with PMA for 72 hours. Subcellular distributions of TM (triangle), PYK2 (arrow), and cofilin (arrow) in THP-1 cells were detected by immunofluorescence and observed by confocal microscopy. DAPI was used to stain the nuclei of THP-1 cells.

cells, which is reflected by increased adherence and the increased expression of surface markers that are associated with macrophage differentiation¹³. To determine the PKC isoform that is responsible for TM's function in PMA-induced THP-1 cells, PKC isoforms, including PKC α , PKC β , PKC δ , PKC ϵ , and PKC θ , were knocked down using specific shRNAs (short-hairpin RNA) prior to PMA treatment, and the characteristics of macrophages were then assayed. First, we used western blot analysis to confirm the knockdown efficiency of each specific shRNA. The knockdown efficiency of these shRNAs in THP-1 cells (1×10^6) that were showed in Fig. 4A. We found that knocking down the PKC δ isoform in THP-1 cells significantly decreased the CD14-positive cell labeling intensity that was induced by PMA treatment relative to the control PMA-treated group (Fig. 4B column 5). Furthermore, p21^{Cip1/WAF1} levels were markedly decreased and PCNA levels were increased in the group in which PKC δ was knocked down prior to PMA treatment (Fig. 4C lane 4), suggesting that PKC δ is the important PKC mediator during PMA-induced THP-1 differentiation. However, knockdown in THP-1 cells using the other PKC α , PKC β , PKC ϵ , and PKC θ shRNAs had no significant inhibitory effects. In addition, PKC δ knockdown strongly inhibited PMA-induced ERK1/2 activation (Fig. 4D lane 3), suggesting that PKC δ is the upstream molecule that mediates ERK1/2 activation in PMA-induced THP-1 cell differentiation. Schwende *et al.* reported that PMA-derived, but not VD3-derived, THP-1 differentiation resulted in the translocation of PKC isoenzymes to membrane fractions¹³. Hence, we hypothesized that TM may act as a scaffold for PKC docking. A co-IP assay was used to verify the interaction between TM and PKC δ in PMA-stimulated THP-1 cells. Western blot analysis showed that no signal was observed in the IgG IP control (Fig. 4E, left), whereas PKC δ was detectable in the anti-TM antibody immunoprecipitated fraction derived from PMA-stimulated THP-1 cells, indicating that there is an interaction between TM and PKC δ in THP-1 cells. In order to further confirm the interaction between TM and PKC δ , immunoprecipitation using goat anti-PKC δ antibody was also done. The data indicated that the co-immunoprecipitated TM was obviously detected in anti-PKC δ antibody immunoprecipitate (Fig. 4E). Additionally, confocal microscopy showed that the PKC δ was predominantly and dispersedly found in the naïve THP-1 cells. PMA may trigger the activation of PKC δ , and make PKC δ colocalized with TM in THP-1 cells (Fig. 4F). These results indicate that PKC δ , which interacts with TM, is the molecule that links TM to ERK1/2 signaling. We therefore suggest that TM may act as a scaffold for PKC δ docking, which could keep PKC δ in the region close to the membrane and activate downstream signaling.

ERK1/2 regulates p21^{Cip1/WAF1} expression and PKC δ interacts with TM in human PBMC. In order to confirm those phenomena which were observed in THP-1 cells, the selected confirmatory experiments were performed using human peripheral blood mononuclear cells (PBMCs). The western blotting results demonstrated that exposing PBMCs to 150 nM PMA for 12–48 hours induced ERK1/2 phosphorylation (Fig. 5A, upper). Additionally, p21^{Cip1/WAF1} expression by PMA markedly increased, blockade of ERK1/2 using PD98059 abrogated the PMA-induced increase in p21^{Cip1/WAF1} levels (Fig. 5A, lower), and suggesting that ERK1/2-mediated signaling played a critical role in PMA-induced p21^{Cip1/WAF1} expression in human PBMCs. A co-IP assay was used to verify the interaction between TM and PKC δ in PMA-stimulated PBMCs. Western blot analysis showed that no signal was observed in the IgG IP control (Fig. 5B, upper), whereas PKC δ was detectable in the anti-TM antibody immunoprecipitated fraction derived from PMA-stimulated PBMCs, indicating that there is an interaction between TM and PKC δ in PBMCs. In order to further confirm the interaction between TM and PKC δ , immunoprecipitation using goat anti-PKC δ antibody was also done. The data indicated that the co-immunoprecipitated TM was obviously detected in anti-PKC δ antibody immunoprecipitate (Fig. 5B, lower). Additionally, confocal microscopy showed that the PMA treatment may trigger the expression of CD68 in PBMCs (Fig. 5C). PKC δ was predominantly and dispersedly found in the naïve PBMCs. PMA may trigger the activation of PKC δ , and make PKC δ colocalized with TM in PBMCs (Fig. 5D). These results indicate that ERK1/2 activation regulates p21^{Cip1/WAF1} expression and PKC δ interacts with TM in PMA-stimulated PBMCs, which is consistent with those results in THP-1 cells.

PKC δ is highly expressed in human atherosclerotic arteries and co-localizes with TM in infiltrated macrophages. To investigate the pathophysiological significance and *in situ* expression of TM and to confirm the evidence shown in *in vitro* studies, atherosclerotic arteries were evaluated using immunohistochemistry. Clinical specimens from patients who underwent CABG (coronary artery bypass grafting) surgery and heart transplantation were obtained. The arrows in the Fig. 5 indicated the internal elastic lamina. There did not have thickened intima or atherosclerotic lesion formation in the normal vessel. In contrast, markedly clarified neointima in both slightly and severely atherosclerotic arteries were observed. Staining with anti-CD68 Ab for identification of infiltrated macrophages showed that less macrophages infiltrated into the vessel walls in the control vessel compare to atherosclerotic vessels. The expression of TM was predominant on endothelium in normal vessel. In contrast, significant inhibition of TM on endothelium was observed in atherosclerotic vessel. The atherosclerotic vessels contain higher levels of PKC δ expression and macrophage infiltration. Furthermore, high power magnification (1000X) revealed strong TM (triangle) expression in neointima-infiltrated CD68-positive macrophages (arrowhead). Strong PKC δ (thick arrow) staining was also detectable (Fig. 6A). We also got the similar presentation in immunofluorescent triple staining (Fig. 6C). These results indicate that PKC δ is highly expressed in human atherosclerotic arteries and that it co-localizes with TM in infiltrated macrophages, suggesting that TM and PKC δ coordinate in macrophages to participate in atherogenesis.

Discussion

This report describes the direct evidence that suggests an important role for endogenous TM in PMA-induced THP-1 cell differentiation, demonstrating that the signaling molecules that mediate macrophage differentiation are regulated by TM. TM is a cell surface-expressed transmembrane glycoprotein. It consists of 557 amino acids, and it contains 5 domains, including a highly charged N-terminal lectin-like domain (D1), a domain with six

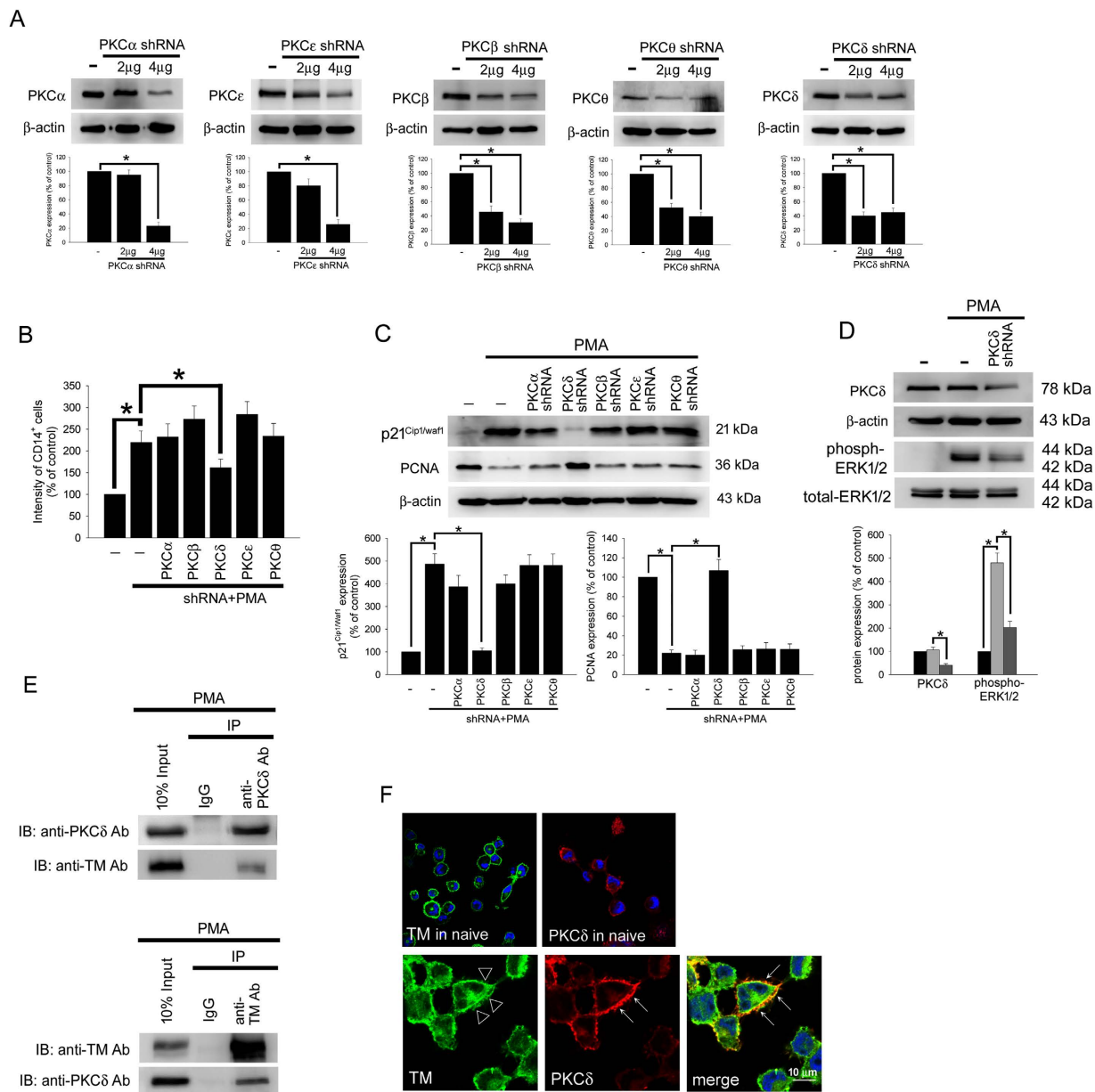


Figure 4. TM regulates THP-1 cell differentiation via the PKC δ -ERK1/2 signaling pathway. (A) THP-1 cells were transfected with 2 or 4 μ g of PKC α , PKC β , PKC δ , PKC ϵ , or PKC θ shRNA for 24 h. Total cell lysates were purified, and knockdown efficiency was assayed using western blot analysis. (B) The THP-1 cells were knocked down by PKC α , PKC β , PKC δ , PKC ϵ , and PKC θ shRNAs for 24 h followed by PMA stimulation for 72 hours. The number of CD14⁺ cells was scored using flow cytometry. Data are expressed as a % of the control, are presented as the mean \pm SD and represent the results of five independent experiments ($n = 5$, $*p < 0.05$ was considered significant). (C) Different sets of THP-1 cells were transfected with 4 μ g of each shRNA for 24 h followed by PMA stimulation for 72 hours. The levels of p21^{Cip1/Waf1} and PCNA were analyzed using western blot analysis. (D) The THP-1 cells were knocked down by PKC δ shRNA for 24 h followed by PMA stimulation for 72 hours. The level of PKC δ and total and phosphorylated ERK1/2 was analyzed using western blot analysis. In western blot analysis, β -actin and total-ERK1/2 were used as loading controls. The density of each band was quantified using densitometry and related protein expression was presented as bar graph. The data are presented as the mean \pm SD, and $*p < 0.05$ was considered significant ($n = 5$). (E) Lysates of THP-1 cells with PMA stimulation were extracted. Left, immunoprecipitated using goat anti-PKC δ or goat IgG control antibodies followed by western blot analysis and detected using goat anti-PKC δ or rabbit anti-TM antibodies. Right, immunoprecipitated using rabbit anti-TM or rabbit IgG control antibodies followed by western blot analysis and detected using rabbit anti-TM or goat anti-PKC δ antibodies. Five independent experiments have been performed ($n = 5$). (F) THP-1 cells were treated without (upper photos) or with (lower photos) PMA for 72 hours. Subcellular distributions of TM (triangle) and PKC δ (arrow) in THP-1 cells were detected by immunofluorescence and observed by confocal microscopy. DAPI was used to stain the nuclei of THP-1 cells.

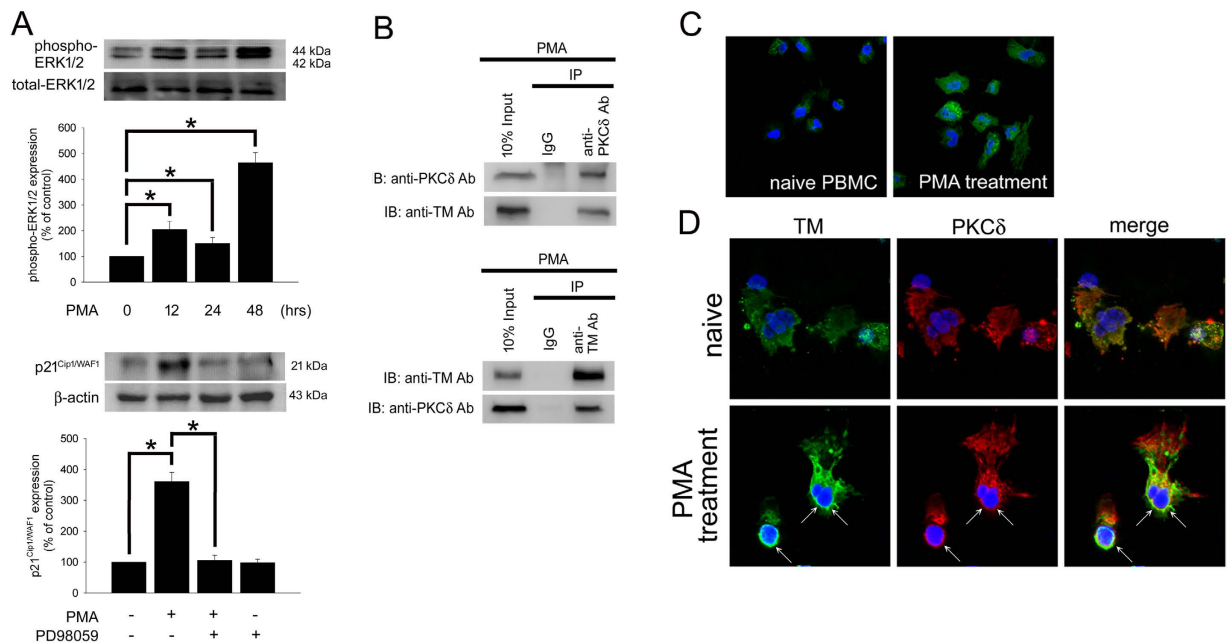


Figure 5. ERK1/2 regulates p21^{Cip1/WAF1} expression and PKC δ interacts with TM in PMA-stimulated PBMCs, which is consistent with those results in THP-1 cells. (A) Human PBMCs were stimulated with 150 nM PMA for 12–48 h. Upper, the expression of phosphorylated ERK1/2 in total cell lysates were assayed using western blot analysis. Lower, human PBMCs were treated with 150 nM PMA, pretreated with 10 μ M PD98059 for 1 h followed by PMA treatment, or treated with PD98059 alone for 48 h. A western blot assay was performed to determine the expression of p21^{Cip1/WAF1}. The total-ERK1/2 and β -actin were used as loading controls. Three independent experiments (PBMCs from 3 voluntary donors) have been performed (n = 3), and representative images have been showed. The density of each band was quantified using densitometry and related protein expression was presented as bar graph. The data are presented as the mean \pm SD, and * p < 0.05 was considered significant. **(B)** Lysates of PBMCs with 150 nM PMA stimulation for 24 hours were extracted. Upper, immunoprecipitated using goat anti-PKC δ or goat IgG control antibodies followed by western blot analysis and detected using goat anti-PKC δ or rabbit anti-TM antibodies. Lower, immunoprecipitated using rabbit anti-TM or rabbit IgG control antibodies followed by western blot analysis and detected using rabbit anti-TM or goat anti-PKC δ antibodies. **(C)** PBMCs were treated with 150 nM PMA for 24 hours. The expression of CD68 in PBMCs was detected by immunofluorescence and observed by confocal microscopy. **(D)** PBMCs were treated without (upper photos) or with (lower photos) PMA for 24 hours. Subcellular distributions of TM (arrow) and PKC δ (arrow) in PBMCs were detected by immunofluorescence and observed by confocal microscopy. DAPI was used to stain the nuclei of PBMCs. Three independent experiments (PBMCs from 3 voluntary donors) have been performed, and representative images were presented.

epidermal growth factor (EGF)-like structures (D2), a serine and threonine-rich domain (D3), a transmembrane domain (D4) and a cytoplasmic domain (D5)¹⁷. Recent evidence has revealed that TM, especially its lectin-like domain, performs potent anti-inflammatory functions independent of its anticoagulant activity, demonstrating a potential therapeutic role for recombinant TM protein for the treatment of inflammatory diseases³⁵. In addition, Cheng *et al.* have reported that TM is implicated in keratinocyte differentiation and wound healing. Primary cultured keratinocytes obtained from TM^{lox/lox}; K5-Cre mice (keratinocyte-specific TM deletion mice) underwent abnormal differentiation in response to calcium stimulation. Downregulation of loricrin and filaggrin indicated poor epidermal differentiation and wound healing were observed in TM^{lox/lox}; K5-Cre mice. Silencing TM expression in human epithelial cells impaired calcium-induced extracellular signal-regulated kinase pathway activation and subsequent keratinocyte differentiation. In addition, local administration of recombinant TM (rTM) improved healing rates in the skin of TM-null mice. Hence they suggested that TM plays a critical role in skin differentiation and wound healing³⁶. Previous studies also focused on the ability of TM to mediate anti-inflammatory effects via its lectin-like domain. The TM lectin-like domain might regulate inflammation by maintaining the integrity of cell-cell interactions and preventing the transmigration of leukocytes³⁷. TM maintains epithelial morphology and promotes cell migration by the direct interaction of its cytoplasmic domain and ezrin which associates with actin filaments³⁸. Additionally, our *in vitro* findings suggested that TM interacts with the actin cytoskeleton and simultaneously interacts with intersectin, further supported a role for TM in cell migration²⁷. The cytoskeleton is a key component that allows cells to maintain proliferation, migration, and differentiation. LIMK1 activates actin depolymerizing factor/cofilin and induces actin reorganization. The phosphorylation of PYK2 and paxillin associate with the focal adhesion complexes formation and cell migration in monocytes^{39,40}. Thus, we predict that TM may interact with ezrin, intersectin, and actin filaments, which result in regulation of cell differentiation.

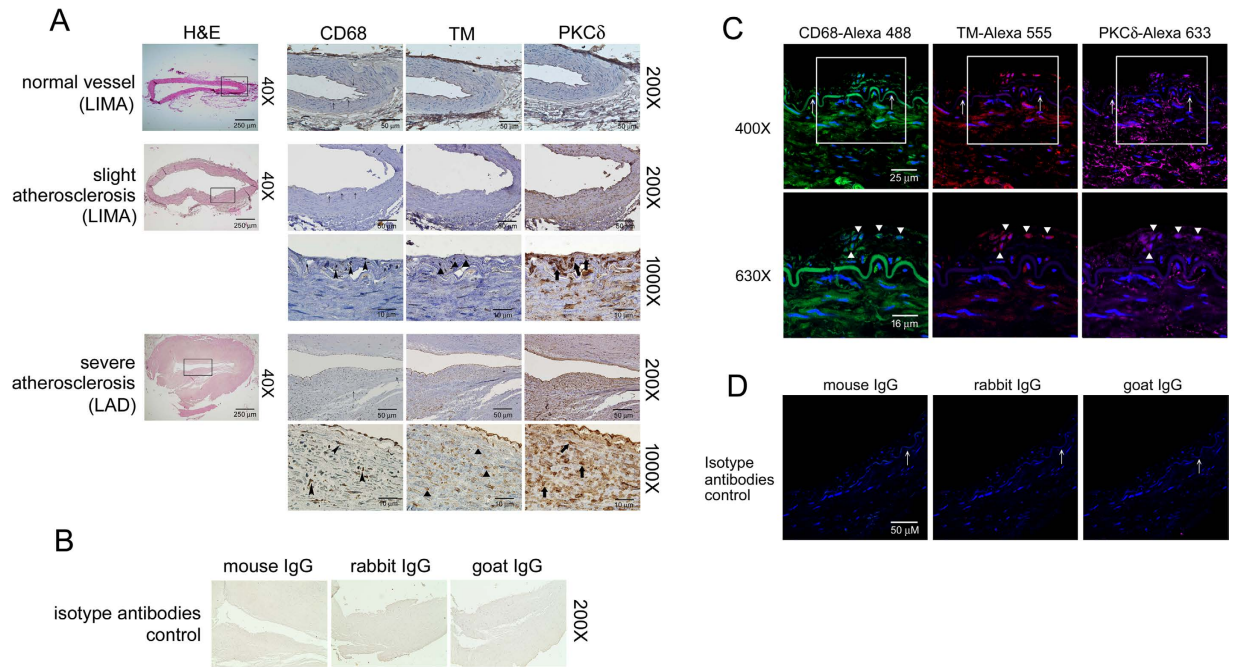


Figure 6. The expression of TM and PKC δ in infiltrated macrophages in human atherosclerotic arteries.

(A) Immunohistochemistry was used to assay the expression of CD68, TM and PKC δ in human LIMA and LAD. The expression of CD68, TM, and PKC δ was determined using specific antibodies, and tissues were counterstained with hematoxylin. CD68 antibodies were used to identify the infiltrated macrophages in vessel walls. H&E staining showed that the intima was thickened in both slightly atherosclerotic LIMA and severely atherosclerotic LAD (black rectangle). Images at 200X and 1000X have been shown. The black arrows indicate the internal elastic lamina. In addition, CD68, TM, and PKC δ ⁺ cells are indicated with black arrowheads, triangles, and thick arrows, respectively. Six human samples (3 for slight atherosclerosis and 3 for severe atherosclerosis) have been analyzed and representative images have been shown. (B) The mouse isotype IgG, rabbit isotype IgG, or goat isotype IgG were used as controls. (C) The expression of CD68, TM and PKC δ in human atherosclerotic vessels were identified using immunofluorescent triple staining. DAPI was used to stain the nuclei of cells. Photos are shown the same regions as 400X magnifications of tissues on slides in the upper column. The white arrows indicate the internal elastic lamina. In addition, images at 630X are shown (white rectangles on 400X slides), and CD68, TM, and PKC δ ⁺ cells are indicated with black triangles. (D) The mouse isotype IgG, rabbit isotype IgG, or goat isotype IgG were used as controls for immunofluorescent staining.

However, the expressions of TM in various monocytic cell lines are differences. As early as 1993, Kizaki K *et al.* had evidenced that TM mRNA levels were induced by 0.1–10 nM of PMA in monocytic, macrophagic and neutrophilic cells differentiated from HL-60 cells⁴¹. Except U937, THP-1 and HL-60 cells expressed high levels of surface TM. Stimulation with LPS or TNF- α up-regulated TM expression by mononuclear phagocytes⁴². Our previous study demonstrated that TM is expressed in monocytes and that its intracellular domain acts as a negative regulator that inhibits cytoskeleton activation in IL-6-mediated THP-1 cell migration. TM siRNA increases IL-6-induced THP-1 cell chemotaxis and migration by activating ERK1/2 and JNK/SAPK signaling²⁷. However, in this study, we showed that TM siRNA decreases PMA-induced THP-1 cell differentiation via the inactivation of ERK1/2 and NK- κ B signaling, indicating a diversity of roles for TM in monocyte functions that depend on the stimuli received by the cell. In 2012, Yang *et al.*²⁸ demonstrated that recombinant human soluble TM (rTM) induced THP-1 cell growth arrest and differentiation via the activation of JNK/c-Jun signaling. In addition, they found that 1,25-(OH)₂D₃ treatment enhanced rTM-induced cell growth arrest and differentiation. They also transfected THP-1 cells with TM plasmid and found that the forced expression of TM increased the percentage of THP-1 cells that expressed CD14, which resulted in the up-regulation of p-JNK, VDR, and C/EBP α in these cells, supporting the idea that TM is a positive regulator of monocytic leukemia cell differentiation. Although recombinant human soluble TM is suggested to be a potent stimulator of monocyte differentiation, the roles of endogenous TM in PMA-induced THP-1 differentiation and its regulatory mechanisms are not yet fully understood. Our pilot study found that TM expression was increased soon after PMA induction; thus, we focused on the roles and underlying mechanisms by which TM regulates these cell processes. We used gain-of-function (HA-TM FL transfection) and loss-of-function (TM siRNA) approaches to define the involvement of TM in PMA-induced THP-1 cell differentiation, and we suggest that TM may act as a scaffold for a direct interaction with PKC δ , which contributes to subsequent ERK1/2 signaling activation and results in THP-1 cell differentiation. Our advanced data (not demonstrated in this text) evidenced that domain 5 (intracellular domain) of TM is involved in PMA-dependent paxillin, cofilin, and LIMK1 signaling pathway that regulate cell differentiation. We are manufacturing the serial deleted constructs to identify the minimal region required for TM interaction

with PKC δ ; using the site-directed mutagenesis technique to provide evidence of the requirement for the peptides in this interaction. If the binding domain of TM may be measured, it could represent a promising approach to prevent inflammation and atherosclerosis in patients via the regulation of TM expression.

During the process of lesion formation and vascular inflammation in atherosclerosis, macrophage differentiation, proliferation, cell growth arrest, and apoptosis *et al.* all are essential for pathogenesis^{43–45}. In early stage of atherosclerosis, macrophages limit lesion progression by phagocytizing oxidized lipoproteins, dead cells, and cellular debris. Unfortunately, the macrophages in advanced lesions contribute to an inappropriate inflammation that can lead to irreversible plaque formation⁴⁵. However, in this complex and gradual process, many potential factors are involved, such as p21^{Cip1/WAF1}, PCNA, G1 cyclin-CDK *et al.* Reduced cell growth is coupled to differentiation. Additionally, the cell cycle inhibitor p21^{Cip1/WAF1} is responsible for the early stages of the differentiation program^{28,29}. p21^{Cip1/WAF1} inhibits cell cycle progression by binding to G1 cyclin-CDK complexes via its N-terminal domain. In addition, p21^{Cip1/WAF1} also binds to PCNA at its C-terminal domain and thereby blocks the ability of PCNA to activate DNA polymerase δ , which is the principal replicative DNA polymerase^{32,46}. Therefore, combined with the previous evidences and our finding in this study, we predict that TM-PKC δ may inhibit cell growth in monocytes. Indeed, we have been studying this important issue *in vitro* study and in cardiac surgery patients.

The transient activation of ERK1/ERK2 is sufficient to induce the expression of p21^{Cip1/WAF1} in G1 phase⁴⁷. Our study demonstrated that HA-TM-FL transfection significantly enhanced PMA-induced cell growth arrest by increasing the level of p21^{Cip1/WAF1} through ERK1/2-NF-kB p65 signaling, which increased the percentage of cells in G0-G1stage cell and promoted differentiation. The PKC isoforms α , β , and δ are implicated in the induction of macrophage differentiation in normal progenitor cells as well as in human and murine myeloid cell lines^{48,49}. M-CSF induced the rapid catalytic activation of PKC- δ and the membrane translocation of phosphorylated PKC- δ in myeloid precursor cells⁵⁰. Schwende *et al.* demonstrated that PMA caused a strong increase in PKC δ and a weak increase in PKC- α , PKC- ϵ , and PKC- ξ expression¹³. The studies described above strongly suggest that PKC δ may be the key molecule that is involved in the TM-associated differentiation of THP-1 cells that is induced by PMA. Consistent with this finding, our data showed that knockdown of the PKC δ isoform in THP-1 cells significantly decreased CD14-positive cell labeling intensity, ERK1/2 activation, and p21^{Cip1/WAF1} levels, suggesting that PKC δ is the important PKC mediator that is the upstream molecule that mediates ERK1/2 activation in PMA-induced THP-1 cell differentiation.

Macrophages participate in intracellular lipid accumulation and foam cell formation in early atherosclerosis lesions⁵. However, uptake of low-density lipoprotein (LDL) by macrophages via scavenger receptors is one of the critical steps in atherogenesis⁵¹. Cholesterol loading of macrophages stimulates the production of inflammatory mediators, such as cytokines and reactive oxygen species, that recruit other cell types and contribute to the development of a complex lesion⁵². The studies described above strongly indicate that macrophage differentiation is an essential process during atherosclerosis development. Therefore, determining the mechanisms by which monocytes differentiate into macrophages is critical to understanding how to prevent atherosclerosis. In the presence of agonists of RXR (retinoid X receptor), a member of the nuclear hormone receptor superfamily, PMA-induced THP-1 cell differentiation was inhibited, suggesting that RXR and its agonists may be useful for therapeutic applications in the future through these anti-atherosclerotic effects⁵³. Similar to our finding, in 1997, Oida *et al.* demonstrated that PMA also increased the expression level of TM in THP-1 cells⁵⁴. However, they also found that incubation with oxLDL resulted in an increase of TM levels in THP-1 cells, but did not induce cells differentiation to the macrophages. Although up-regulation of TM in PMA-stimulated THP-1 cells had been demonstrated, here we hypothesized that TM is a key regulator of PMA-induced THP-1 cell differentiation. We further studied TM's regulating mechanisms in detail, which may be helpful for understanding the atherosclerotic effect of endogenous TM on monocyte differentiation and for the development of therapeutic applications in the further.

In conclusion, the schematic diagram shown in Fig. 7 summarizes the mechanism by which TM contributes to the PMA-mediated differentiation of THP-1 cells. TM expression is first increased when THP-1 cells are exposed to PMA. TM then acts as a scaffold for PKC δ docking, which keeps PKC δ in the region close to the membrane and promotes subsequent ERK1/2 activation. On the one hand, ERK1/2 activation enhances the expression of the cell cycle inhibitor p21^{Cip1/WAF1} via NF-kB p65 signaling, which causes cell cycle arrest and promotes differentiation. ERK1/2 activation participates in the phosphorylation of paxillin, cofilin, LIMK1, and PYK2, which interact with TM to mediate cytoskeletal remodeling to promote differentiation. The data strongly suggests that the TM expression participates in PMA-induced macrophage differentiation, and provides a novel view of the role of TM in macrophage differentiation during the development of atherosclerosis.

Methods

Cell culture and differentiation. A human pro-myelomonocytic cell line, THP-1 cells, were obtained from the American Type Culture Collection (ATCC, VA, USA) and grown in RPMI 1640 medium (Thermo-Fisher Scientific Inc, CA, USA) with 2 mM L-glutamate, 4.5 g/L glucose, 10 mmol/L HEPES, 1.0 mmol/L sodium pyruvate, 10% fetal bovine serum, and 1% antibiotic-antimycotic mixture. Cell density was maintained between 5×10^4 and 8×10^5 viable cells/mL, and the medium was refreshed every 48–72 hours. The cells were differentiated into a macrophage-like phenotype by incubating them with 150 nM PMA in complete medium for 72 hours at 37°C in 5% CO₂.

Extraction and treatment of human peripheral blood mononuclear cells. Human total PBMCs were isolated from 50 ml peripheral blood of healthy young human volunteers by density gradient centrifugation with Histopaque-1077 (density 1.077 g/ml; Sigma, MO, USA) according to the user instrument. Extracted PBMCs were plated in RPMI 1640 medium with supplements (2 mM L-glutamate, 4.5 g/L glucose, 10 mmol/L HEPES, 1.0 mmol/L sodium pyruvate, 10% fetal bovine serum, and 1% antibiotic-antimycotic mixture) on cultured plates at 37°C in a 5% CO₂ incubator for 2 hours, then treated cells with 150 nM PMA and performed subsequent studies.

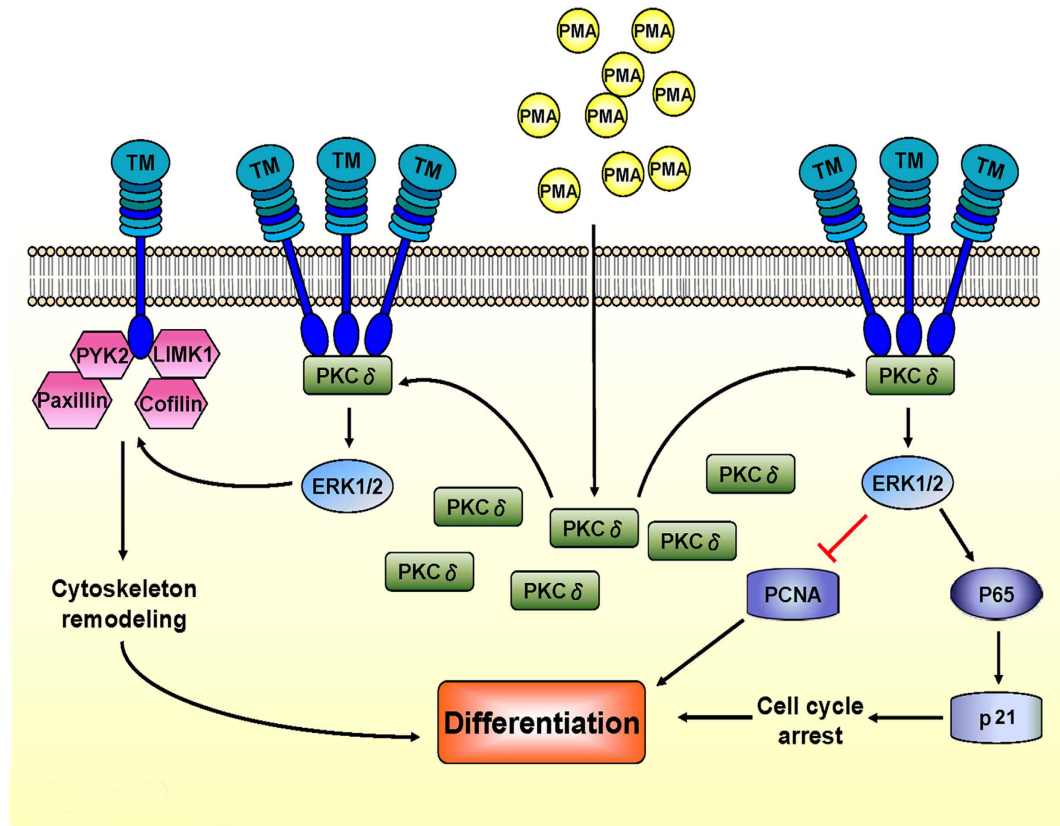


Figure 7. Mechanism by which TM contributes to PMA-mediated differentiation in THP-1 cells. TM expression is increased soon after PMA induction in THP-1 cells. TM may regulate PMA-induced THP-1 cell differentiation via a direct interaction with PKC δ . TM acts as a scaffold for PKC δ docking, which keeps PKC δ in the region close to the membrane and promotes subsequent ERK1/2 activation. ERK1/2 activation subsequently enhances the expression of cell cycle inhibitor p21^{Cip1/WAF1} via NF- κ B p65 signaling, which causes cell cycle arrest and promotes differentiation. On the other hand, ERK1/2 activation participates in the phosphorylation of paxillin, cofilin, LIMK1, and PYK2, which interact with TM and mediate cytoskeleton remodeling to promote differentiation.

Knockdown of TM gene expression by siRNA transfection. The knockdown of TM gene expression was achieved by siRNA transfection. THP-1 cells (1×10^6) were suspended in 2.5 mL of serum-free medium and transfected with 25 μ M of TM siRNA duplexes (Invitrogen Catalog THBD-HSS110719, 110721, 186320, NY, USA) for 6 hours using Lipofectamine[®] RNAiMAX (Invitrogen, Carlsbad, CA, USA) according to the manufacturer's instructions. Then, the cells were resuspended in complete medium and analyzed for siRNA knockdown efficiency 24 h after transfection using flow cytometry and western blot analysis.

Knockdown of PKC gene expression by shRNA electroporation. shRNAs against human PKC α , PKC β II, PKC δ , PKC ϵ , and PKC θ were purchased from National RNAi Core Facility User Committee Academia Sinica, Taipei, Taiwan. THP-1 cells were transfected with shRNAs via electroporation using the Neon transfection system (Invitrogen, Carlsbad, CA, USA) according to the manufacturer's instructions. A total of 1×10^6 cells were transfected with 2 or 4 μ g of each shRNA plasmid and then cultured with complete medium without antibiotic-antimycotic mixture at 37 $^{\circ}$ C in 5% CO $_2$. The cells were analyzed for shRNA knockdown efficiency 24 h after electroporation using western blot analysis.

Construction and overexpression of HA-tagged TM full-length expression vectors in electroporated THP-1 cells. The pCDNA3.1/V5-His-TM-FL plasmid, which contains a segment of the TM open reading frame, was a gift from Professor Yu-Jia Chang, Taipei medical University, Taiwan. For the construction of the influenza hemagglutinin (HA) epitope-tagged full-length TM expression plasmid (HA-TM FL), the pCDNA3.1/V5-His-TM plasmid was first digested with the SacI and XhoI enzymes, filled in with Klenow, and subsequently cloned in-frame into the SmaI sites of the pXJN-HA vector, which contains the chick β -globin intron downstream (3') of the CMV promoter. THP-1 cells were transfected with HA-TM FL plasmids via electroporation using the Neon transfection system (Invitrogen, Carlsbad, CA, USA) according to the manufacturer's instructions. A total of 1×10^6 cells were transfected with 2 μ g of HA-TM FL plasmid. The cells were analyzed for overexpression 24 h after electroporation.

Macrophage identification by Liu and immunofluorescence staining. The PMA-treated THP-1 cells or PBMCs (1×10^5) were rinsed with PBS, fixed in 4% paraformaldehyde, and spun onto glass slides using a Shandon Cytospin 4 Cyto centrifuge (Thermo Scientific, Pittsburgh, PA, USA). The macrophages were first identified using Liu staining and examined using an Axio Imager A1 Microscope (Carl Zeiss Micro Imaging Inc., Thornwood, NY, USA). The slides were stained using either PE-conjugated mouse anti-human CD14 (25–0149, eBioscience, San Diego, CA, USA) or FITC-conjugated mouse anti-human CD68 (11–0689, eBioscience), and nuclei were identified using Hoechst 33258 (Sigma, St. Louis, MO, USA). Images were obtained using an Axio Imager A1 microscope (Carl Zeiss Micro Imaging Inc., Thornwood, NY, USA).

Flow cytometry for macrophage cell surface marker analysis. The identification and characterization of THP-1 differentiation were also performed using flow cytometry. THP-1 cells were harvested and incubated with PE-conjugated mouse anti-human CD14 (25–0149, eBioscience), FITC-conjugated mouse anti-human CD68 (11–0689, eBioscience), or a mouse IgM/IgG2a isotype control (DakoCytomation, Produktionsvej, Glostrup, Denmark) for 60 min. After washing the cells with buffer (phosphate-buffered saline containing 0.1% bovine serum albumin and 0.1% sodium azide), the expression of the cell surface markers CD14 and CD68 was analyzed using flow cytometry on a FACSCalibur™ (BD Biosciences, Franklin Lakes, New Jersey, USA).

Cell cycle analysis by DNA content using flow cytometry. A total of 2×10^6 THP-1 cells were fixed with 70% ethanol at 4 °C for at least 24 hours. Cells were washed three times with cold PBS and resuspended in PI staining solution containing 25 µg/ml PI, 40 µg/ml RNase, and 0.3% Tween-20 at room temperature for 30 minutes. Finally, cell DNA contents were analyzed using flow cytometry on a FACSCalibur™ (BD Biosciences, Franklin Lakes, New Jersey, USA).

Western blot analysis. We placed 3×10^6 cells in 10 cm dish for western blot analysis. We collected the suspended and attached THP-1 cells, and the total cell lysates were extracted. Protein concentrations were determined using a Bio-Rad Protein Assay Kit (BioRad Inc., CA, USA), with BSA used as the standard. For each blot, approximately 50 µg of total protein was fractionated by SDS-PAGE and transferred to a PVDF (polyvinylidene difluoride) membrane. The membranes were respectively probed with rabbit anti-human TM (TA307719, OriGene Technologies, Inc, Rockville, MD, USA), rabbit anti-p21^{Cip1/WAF1} (#2947, Cell Signaling, Danvers, CA, USA), rabbit anti-PCNA (sc-7907, Santa Cruz biotechnology, Santa Cruz, CA, USA), mouse anti-phospho-p44/42 MAPK (Erk1/2) (Thr202/Tyr204) (#9106, Cell Signaling, Danvers, CA, USA), rabbit anti-p44/42 MAPK (Erk1/2) (#9102, Cell Signaling, Danvers, CA, USA), rabbit anti-phospho-NF-κB p65 (Ser536) (#3033, Cell Signaling, Danvers, CA, USA), rabbit anti-Paxillin (phospho Y31)(ab32115, Abcam, MA, USA), rabbit anti-Paxillin (ab32084), rabbit anti-Cofilin (phospho S3)(ab47281, Abcam, MA, USA), rabbit anti-Cofilin (ab54532, Abcam, MA, USA), rabbit anti-LIM Kinase 1 (phospho T508)(ab38508, Abcam, MA, USA), rabbit anti-LIM Kinase 1 (ab87971, Abcam, MA, USA), rabbit anti-PYK2 (phospho Y881)(ab4801, Abcam, MA, USA), rabbit anti-PYK2 (ab32571, Abcam, MA, USA), mouse anti-PKC α (sc-8393, Santa Cruz Biotechnology, Santa Cruz, CA, USA), rabbit anti-PKC βII (sc-210, Santa Cruz Biotechnology, Santa Cruz, CA, USA), goat anti-PKC θ (sc-1875, Santa Cruz Biotechnology, Santa Cruz, CA, USA), goat anti-PKC δ (sc-937-G, Santa Cruz Biotechnology, Santa Cruz, CA, USA), and rabbit anti-PKC ε (sc-214, Santa Cruz Biotechnology, Santa Cruz, CA, USA) antibodies. The membranes were then incubated with horseradish peroxidase (HRP)-conjugated goat anti-rabbit IgG antibodies (Merck Millipore, Darmstadt, Germany), HRP-conjugated goat anti-mouse IgG antibodies (Merck Millipore, Darmstadt, Germany) or HRP-conjugated donkey anti-goat IgG antibodies (Amersham, Arlington Heights, IL, USA). The proteins were visualized using an enhanced chemiluminescence (ECL) detection kit (Amersham Biosciences, NJ, USA) and scanned by Odyssey Imaging System (LI-COR, Inc., Lincoln, NE, USA).

Immunoprecipitation. THP-1 cells transfected with either TM siRNA or PKCs shRNA and untransfected controls were lysed in buffer containing 150 mM NaCl, 50 mM Tris-HCl (pH 7.4), 1% NP-40, and 1X protease inhibitor cocktail (Sigma, MO, USA). Lysed cells were placed on ice for 30 minutes and then centrifuged at $10,000 \times g$ for 30 minutes to remove cell debris. Approximately 500 µg of protein extract was pre-cleaned with 20 µL of a 50% protein A/G suspension mixture (protein A: BioRad, Inc., CA; protein G: Amersham, IL, USA). Pre-cleaned lysates were immunoreacted with rabbit anti-human TM antibody (TA307719, OriGene Technologies, Inc, Rockville, MD, USA) or rabbit IgG (Sigma, St. Louis, MO, USA) at 4 °C for 16 h and then immunoprecipitated by adding 50 µL of a 50% protein A/G sepharose mixture at 4 °C for 1.5 hrs. The beads were washed three times with ice-cold lysis buffer, and the bound proteins were eluted with 2X SDS-PAGE loading buffer and subjected to western blot analysis.

Human artery collection and immunohistochemical/immunofluorescent staining. Human left internal mammary arteries (LIMA) were obtained from patients who underwent coronary artery bypass graft (CABG) surgery, and left coronary arteries (LAD) were obtained from the patients who underwent heart transplantation. The Ethics Committee of Tri-Service General Hospital approved this study (TSGHIRB 100-05-232), which conformed to the requirements of the Declaration of Helsinki, and all patients gave informed consent prior to all procedures. Immunohistochemical staining was performed on serial and 5 µm-thick paraffin-embedded cross-sections of LIMA and LAD using mouse anti-human CD68 (sc-20060, Santa Cruz biotechnology, Santa Cruz, CA, USA), rabbit anti-human TM, (TA307719, OriGene Technologies, Inc, Rockville, MD, USA), and goat anti-human PKC δ (sc-937-G, Santa Cruz biotechnology, Santa Cruz, CA, USA) antibodies. The anti-mouse, rabbit, and goat IgG peroxidase-conjugated or Alexa Fluor-conjugated secondary antibodies were purchased from Amersham (Arlington Heights, IL, USA) or Invitrogen (Carlsbad, CA, USA). The nuclei were counterstained with hematoxylin or DAPI. The mouse IgG, rabbit IgG, or goat IgG isotype antibodies were used as controls. One of the

serial sections was assayed using hematoxylin and eosin (H&E) to determine the vessel morphology. Images were acquired using Axio Imager A1 microscope (Carl Zeiss Micro Imaging Inc., Thornwood, NY, USA).

Statistical analyses. In this experiment, we performed each test for five times ($n = 5$), including *in vitro* cell experiments. The amount of protein expression in western blot analysis was quantified using ImageQuant TL software (version 7.0; GE Healthcare Life Sciences, Marlborough, MA, USA). The β -actin, total-ERK1/2, or lamin B1 were used for normal loading controls/normalization. The ratio of the abundance of the target protein to the normal loading control is used to quantify the amount of the target protein in each sample. The expression level of target protein was presented as % of control group or fold of control group. Statistical analysis was performed using the SigmaStat software (version 3.5; SPSS, Chicago, IL, USA). Between groups analysis of summary statistic was performed using Student's t-tests and one- or two-way ANOVA followed by Dunnett's test. Value was expressed as the means \pm SD and statistical significant was set at $P < 0.05$.

References

- Syrovets, T., Thillet, J., Chapman, M. J. & Simmet, T. Lipoprotein(a) is a potent chemoattractant for human peripheral monocytes. *Blood* **90**, 2027–2036 (1997).
- Xaus, J. *et al.* Molecular mechanisms involved in macrophage survival, proliferation, activation or apoptosis. *Immunobiology* **204**, 543–550, doi: 10.1078/0171-2985-00091 (2001).
- Glass, C. K. & Witztum, J. L. Atherosclerosis. the road ahead. *Cell* **104**, 503–516 (2001).
- Lusis, A. J. Atherosclerosis. *Nature* **407**, 233–241, doi: 10.1038/35025203 (2000).
- Takahashi, K., Takeya, M. & Sakashita, N. Multifunctional roles of macrophages in the development and progression of atherosclerosis in humans and experimental animals. *Medical electron microscopy: official journal of the Clinical Electron Microscopy Society of Japan* **35**, 179–203 (2002).
- Fuhrman, B., Partoush, A., Volkova, N. & Aviram, M. Ox-LDL induces monocyte-to-macrophage differentiation *in vivo*: Possible role for the macrophage colony stimulating factor receptor (M-CSF-R). *Atherosclerosis* **196**, 598–607, doi: 10.1016/j.atherosclerosis.2007.06.026 (2008).
- Qiao, J. H. *et al.* Role of macrophage colony-stimulating factor in atherosclerosis: studies of osteopetrotic mice. *The American journal of pathology* **150**, 1687–1699 (1997).
- Yamaguchi, H., Haranaga, S., Widen, R., Friedman, H. & Yamamoto, Y. Chlamydia pneumoniae infection induces differentiation of monocytes into macrophages. *Infection and immunity* **70**, 2392–2398 (2002).
- Ross, R. Atherosclerosis—an inflammatory disease. *The New England journal of medicine* **340**, 115–126 (1999).
- Libby, P. *et al.* Macrophages and atherosclerotic plaque stability. *Current opinion in lipidology* **7**, 330–335 (1996).
- Smith, J. D. *et al.* Decreased atherosclerosis in mice deficient in both macrophage colony-stimulating factor (op) and apolipoprotein E. *Proceedings of the National Academy of Sciences of the United States of America* **92**, 8264–8268 (1995).
- Steinberg, D. Low density lipoprotein oxidation and its pathobiological significance. *The Journal of biological chemistry* **272**, 20963–20966 (1997).
- Schwende, H., Fitzke, E., Ambs, P. & Dieter, P. Differences in the state of differentiation of THP-1 cells induced by phorbol ester and 1,25-dihydroxyvitamin D3. *Journal of leukocyte biology* **59**, 555–561 (1996).
- Newton, A. C. Protein kinase C: structure, function, and regulation. *The Journal of biological chemistry* **270**, 28495–28498 (1995).
- Hug, H. & Sarre, T. F. Protein kinase C isoenzymes: divergence in signal transduction? *The Biochemical journal* **291** (Pt 2), 329–343 (1993).
- Stabel, S. Protein kinase C—an enzyme and its relatives. *Seminars in cancer biology* **5**, 277–284 (1994).
- Suzuki, K. *et al.* Structure and expression of human thrombomodulin, a thrombin receptor on endothelium acting as a cofactor for protein C activation. *The EMBO journal* **6**, 1891–1897 (1987).
- Lentz, S. R., Chen, Y. & Sadler, J. E. Sequences required for thrombomodulin cofactor activity within the fourth epidermal growth factor-like domain of human thrombomodulin. *The Journal of biological chemistry* **268**, 15312–15317 (1993).
- Senet, P., Peyri, N., Berard, M., Dubertret, L. & Boffa, M. C. Thrombomodulin, a functional surface protein on human keratinocytes, is regulated by retinoic acid. *Archives of dermatological research* **289**, 151–157 (1997).
- Suzuki, K., Nishioka, J., Hayashi, T. & Kosaka, Y. Functionally active thrombomodulin is present in human platelets. *Journal of biochemistry* **104**, 628–632 (1988).
- McCachren, S. S., Diggs, J., Weinberg, J. B. & Dittman, W. A. Thrombomodulin expression by human blood monocytes and by human synovial tissue lining macrophages. *Blood* **78**, 3128–3132 (1991).
- Shi, C. S. *et al.* Evidence of human thrombomodulin domain as a novel angiogenic factor. *Circulation* **111**, 1627–1636, doi: 10.1161/01.CIR.0000160364.05405.B5 (2005).
- Huang, H. C. *et al.* Thrombomodulin-mediated cell adhesion: involvement of its lectin-like domain. *The Journal of biological chemistry* **278**, 46750–46759 (2003).
- Esmon, C. T. Coagulation and inflammation. *Journal of endotoxin research* **9**, 192–198 (2003).
- Van de Wouwer, M., Collen, D. & Conway, E. M. Thrombomodulin-protein C-EPCR system: integrated to regulate coagulation and inflammation. *Arteriosclerosis, thrombosis, and vascular biology* **24**, 1374–1383 (2004).
- Tsai, C. S. *et al.* Expression of thrombomodulin on monocytes is associated with early outcomes in patients with coronary artery bypass graft surgery. *Shock* **34**, 31–39 (2010).
- Lin, Y. W. *et al.* The C-Terminal Domain of Thrombomodulin Regulates Monocyte Migration with Interleukin-6 Stimulation. *Eur J Inflamm* **12**, 27–39 (2014).
- Yang, J., Ikezoe, T., Nishioka, C., Honda, G. & Yokoyama, A. Thrombomodulin-induced differentiation of acute myelomonocytic leukemia cells via JNK signaling. *Leukemia research* **36**, 625–633 (2012).
- Andres, V. & Walsh, K. Myogenin expression, cell cycle withdrawal, and phenotypic differentiation are temporally separable events that precede cell fusion upon myogenesis. *The Journal of cell biology* **132**, 657–666 (1996).
- Halevy, O. *et al.* Correlation of terminal cell cycle arrest of skeletal muscle with induction of p21 by MyoD. *Science* **267**, 1018–1021 (1995).
- Chen, J., Jackson, P. K., Kirschner, M. W. & Dutta, A. Separate domains of p21 involved in the inhibition of Cdk kinase and PCNA. *Nature* **374**, 386–388 (1995).
- Waga, S., Hannon, G. J., Beach, D. & Stillman, B. The p21 inhibitor of cyclin-dependent kinases controls DNA replication by interaction with PCNA. *Nature* **369**, 574–578 (1994).
- Sun, J., Ramnath, R. D., Zhi, L., Tamizhselvi, R. & Bhatia, M. Substance P enhances NF- κ B transactivation and chemokine response in murine macrophages via ERK1/2 and p38 MAPK signaling pathways. *American journal of physiology. Cell physiology* **294**, C1586–1596 (2008).
- Provenzano, P. P. & Keely, P. J. Mechanical signaling through the cytoskeleton regulates cell proliferation by coordinated focal adhesion and Rho GTPase signaling. *Journal of cell science* **124**, 1195–1205 (2011).

35. Shi, C. S. *et al.* Lectin-like domain of thrombomodulin binds to its specific ligand Lewis Y antigen and neutralizes lipopolysaccharide-induced inflammatory response. *Blood* **112**, 3661–3670 (2008).
36. Cheng, T. L. *et al.* Thrombomodulin regulates keratinocyte differentiation and promotes wound healing. *The Journal of investigative dermatology* **133**, 1638–1645 (2013).
37. Koutsi, A., Papapanagiotou, A. & Papavassiliou, A. G. Thrombomodulin: from haemostasis to inflammation and tumourigenesis. *The international journal of biochemistry & cell biology* **40**, 1669–1673 (2008).
38. Hsu, Y. Y. *et al.* Thrombomodulin is an ezrin-interacting protein that controls epithelial morphology and promotes collective cell migration. *FASEB J* **26**, 3440–3452 (2012).
39. Liu, S. *et al.* Binding of paxillin to alpha4 integrins modifies integrin-dependent biological responses. *Nature* **402**, 676–681, doi: 10.1038/45264 (1999).
40. Kintscher, U. *et al.* Angiotensin II induces migration and Pyk2/paxillin phosphorylation of human monocytes. *Hypertension* **37**, 587–593 (2001).
41. Kizaki, K., Naito, S., Horie, S., Ishii, H. & Kazama, M. Different thrombomodulin induction in monocytic, macrophagic and neutrophilic cells differentiated from HL-60 cells. *Biochem Biophys Res Commun* **193**, 175–181, doi: 10.1006/bbrc.1993.1606 (1993).
42. Grey, S. T. & Hancock, W. W. A physiologic anti-inflammatory pathway based on thrombomodulin expression and generation of activated protein C by human mononuclear phagocytes. *J Immunol* **156**, 2256–2263 (1996).
43. Andres, V., Pello, O. M. & Silvestre-Roig, C. Macrophage proliferation and apoptosis in atherosclerosis. *Current opinion in lipidology* **23**, 429–438 (2012).
44. Robbins, C. S. *et al.* Local proliferation dominates lesional macrophage accumulation in atherosclerosis. *Nat Med* **19**, 1166–1172 (2013).
45. Rosenfeld, M. E. Macrophage proliferation in atherosclerosis: an historical perspective. *Arteriosclerosis, thrombosis, and vascular biology* **34**, e21–22 (2014).
46. Sherr, C. J. & Roberts, J. M. Inhibitors of mammalian G1 cyclin-dependent kinases. *Genes & development* **9**, 1149–1163 (1995).
47. Bottazzi, M. E., Zhu, X., Bohmer, R. M. & Assoian, R. K. Regulation of p21(cip1) expression by growth factors and the extracellular matrix reveals a role for transient ERK activity in G1 phase. *The Journal of cell biology* **146**, 1255–1264 (1999).
48. Macfarlane, D. E. & Manzel, L. Activation of beta-isozyme of protein kinase C (PKC beta) is necessary and sufficient for phorbol ester-induced differentiation of HL-60 promyelocytes. Studies with PKC beta-defective PET mutant. *The Journal of biological chemistry* **269**, 4327–4331 (1994).
49. Mischak, H. *et al.* Phorbol ester-induced myeloid differentiation is mediated by protein kinase C-alpha and -delta and not by protein kinase C-beta II, -epsilon, -zeta, and -eta. *The Journal of biological chemistry* **268**, 20110–20115 (1993).
50. Junttila, I., Bourette, R. P., Rohrschneider, L. R. & Silvennoinen, O. M-CSF induced differentiation of myeloid precursor cells involves activation of PKC-delta and expression of Pkare. *Journal of leukocyte biology* **73**, 281–288 (2003).
51. Lin, C. S. *et al.* PKCdelta signalling regulates SR-A and CD36 expression and foam cell formation. *Cardiovascular research* **95**, 346–355 (2012).
52. Hansson, G. K., Libby, P., Schonbeck, U. & Yan, Z. Q. Innate and adaptive immunity in the pathogenesis of atherosclerosis. *Circulation research* **91**, 281–291 (2002).
53. Zhou, L. *et al.* Retinoid X receptor agonists inhibit phorbol-12-myristate-13-acetate (PMA)-induced differentiation of monocytic THP-1 cells into macrophages. *Molecular and cellular biochemistry* **335**, 283–289 (2010).
54. Oida, K. *et al.* Effect of oxidized low density lipoprotein on thrombomodulin expression by THP-1 cells. *Thromb Haemost* **78**, 1228–1233 (1997).

Acknowledgements

We thank Wei-Li Chang for excellent technical assistance. This work was supported by National Ministry of Science and Technology (MOST 103-2314-B-016-022-MY3) and by Tri-service General Hospital (TSGH-C102-028, TSGH-C103-028-013, DV103-04 and DV104-08) in Taiwan.

Author Contributions

C.S. Tsai, Y.W. Lin and F.Y. Lin conceived of the project, designed and performed experiments and analysed the data. Y.T. Tsai, H. Jeng and C.S. Lin performed experiments. C.Y. Huang, C.M. Shih, N.W. Tsao and C.C. Shih contributed to the study and experimental design as well as data analysis. This manuscript was written by Y.W. Lin and F.Y. Lin. All authors reviewed the manuscript.

Additional Information

Competing financial interests: The authors declare no competing financial interests.

How to cite this article: Tsai, C.-S. *et al.* Thrombomodulin regulates monocyte differentiation via PKC δ and ERK1/2 pathway *in vitro* and in atherosclerotic artery. *Sci. Rep.* **6**, 38421; doi: 10.1038/srep38421 (2016).

Publisher's note: Springer Nature remains neutral with regard to jurisdictional claims in published maps and institutional affiliations.



This work is licensed under a Creative Commons Attribution 4.0 International License. The images or other third party material in this article are included in the article's Creative Commons license, unless indicated otherwise in the credit line; if the material is not included under the Creative Commons license, users will need to obtain permission from the license holder to reproduce the material. To view a copy of this license, visit <http://creativecommons.org/licenses/by/4.0/>

© The Author(s) 2016